

PHYSICAL OPTICS

Conference materials

UDC 621.373.8

DOI: <https://doi.org/10.18721/JPM.163.201>

Emission linewidth and α -factor of 1.3 μm -range vertical cavity surface emitting laser based on InGaAs/InAlGaAs superlattice

Ya.N. Kovach^{1,2}✉, S.A. Blokhin¹, M.A. Bobrov¹, A.A. Blokhin¹,
N.A. Maleev¹, A.G. Kuzmenkov¹, A.G. Gladyshev², I.I. Novikov²,
L.Ya. Karachinsky², K.O. Voropaev³, A.Yu. Egorov⁴, V.M. Ustinov¹

¹ Ioffe Institute, St. Petersburg, Russia;

² ITMO University, St. Petersburg, Russia;

³ JSC OKB-Planeta, Veliky Novgorod, Russia;

⁴ Connector Optics LLC, St. Petersburg, Russia

✉ j-n-kovach@itmo.ru

Abstract. Static, spectral and linewidth measurements of 1.3 μm -range vertical-cavity surface-emitting lasers based on InGaAs/InAlGaAs superlattice are presented. Minimum emission linewidth about 40-45 MHz was obtained at output power of ~ 3.3 mW and operating current of ~ 8 mA using the Fabry-Perot interferometer method. During a further increase in the output optical power the emission linewidth broadening could be observed due to the rise of a laser internal temperature (self-heating). Based on the analysis of the internal optical losses and internal quantum efficiency the linewidth enhancement factor (α -factor) was evaluated at about 7.7–9 depending on population inversion factor of 2–1.5.

Keywords: vertical-cavity surface-emitting laser, superlattice, wafer fusion, linewidth, α -factor

Funding: The authors from ITMO University acknowledge support in part by Advanced Engineering Schools Federal Project for the optical spectra experiments and in part by the Ministry of Science and Higher Education of the Russian Federation, the research project 2019–1442, for the static characteristic and polarization measurements. S.A. Blokhin acknowledges support for laser emission linewidth measurements from RFBR project 20-52-12006.

Citation: Kovach Ya.N., Blokhin S.A., Bobrov M.A., Blokhin A.A., Maleev N.A., Kuzmenkov A.G., Gladyshev A.G., Novikov I.I., Karachinsky L.Ya., Voropaev K.O., Egorov A.Yu., Ustinov V.M., Emission linewidth and α -factor of 1.3 μm -range vertical cavity surface emitting laser based on InGaAs/InAlGaAs superlattice, St. Petersburg State Polytechnical University Journal. Physics and Mathematics. 16 (3.2) (2023) 9–15. DOI: <https://doi.org/10.18721/JPM.163.201>

This is an open access article under the CC BY-NC 4.0 license (<https://creativecommons.org/licenses/by-nc/4.0/>)

Материалы конференции

УДК 621.373.8

DOI: <https://doi.org/10.18721/JPM.163.201>

Ширина линии излучения и α -фактор вертикально-излучающего лазера спектрального диапазона 1.3 мкм на основе сверхрешетки InGaAs/InAlGaAs

Я.Н. Ковач^{1,2}✉, С.А. Блохин¹, М.А. Бобров¹, А.А. Блохин¹,
Н.А. Малеев¹, А.Г. Кузьменков¹, А.Г. Гладышев², И.И. Новиков²,
Л.Я. Карачинский², К.О. Воропаев³, А.Ю. Егоров⁴, В.М. Устинов¹

¹ Физико-технический институт им. А.Ф. Иоффе РАН, Санкт-Петербург, Россия;

² Университет ИТМО, Санкт-Петербург, Россия;

³ АО «ОКБ-Планета», Великий Новгород, Россия;

⁴ ООО «Коннектор Оптикс», Санкт-Петербург, Россия

✉ j-n-kovach@itmo.ru

Аннотация. В работе представлены результаты измерений статических и спектральных характеристик вертикально-излучающего лазера спектрального диапазона 1.3 мкм на основе сверхрешетки InGaAs/InAlGaAs. Минимальное значение ширины линии излучения, измеренное с помощью Фабри-Перо интерферометра, составило 40-45 МГц при выходной оптической мощности $\sim 3,3$ мВт и рабочем токе ~ 8 мА. При дальнейшем повышении выходной мощности наблюдается уширение линии излучения из-за роста внутренней температуры лазера (саморазогрев с током). Анализ внутренних оптических потерь и эффективности токовой инжекции позволил оценить значение α -фактора на уровне 7.7-9 в зависимости от значения фактора инверсной заселенности 2-1.5.

Ключевые слова: вертикально-излучающий лазер, сверхрешетка, технология спекание пластин, ширина линии, α -фактор

Финансирование: Работа авторов из Университета ИТМО выполнена при поддержке федерального проекта «Передовые инженерные школы» в части исследований оптических спектров, а также при поддержке Министерства науки и высшего образования Российской Федерации, проект тематики научных исследований № 2019-1442 в части ряда исследований статических и поляризационных характеристик. С.А. Блохин выражает благодарность РФФИ № 20-52-12006 в части измерений ширины линии излучения лазера.

Ссылка при цитировании: Ковач Я.Н., Блохин С.А., Бобров М.А., Блохин А.А., Малеев Н.А., Кузьменков А.Г., Гладышев А.Г., Новиков И.И., Карачинский Л.Я., Воропаев К.О., Егоров А.Ю., Устинов В.М., Ширина линии излучения и α -фактор вертикально-излучающего лазера спектрального диапазона 1.3 мкм на основе сверхрешетки InGaAs/InAlGaAs // Научно-технические ведомости СПбГПУ. Физико-математические науки. 2023. Т. 16. № 3.2. С. 9–15. DOI: <https://doi.org/10.18721/JPM.163.201>

Статья открытого доступа, распространяемая по лицензии CC BY-NC 4.0 (<https://creativecommons.org/licenses/by-nc/4.0/>)

Introduction

Today vertical-cavity surface-emitting lasers (VCSELs) and VCSEL-based matrixes are used in optical data communication systems, industrial heating, 3D sensing for consumer electronics, and LIDAR object recognition [1]. Recently, much attention has been paid to the possible implementation of single-mode VCSELs for optical spectroscopy and real-time analysis of industrial gases. However, the development of long-wavelength VCSELs is associated with a number of fundamental problems of the material systems InAlGaAs-GaAs and InAlGaAsP-InP. Today, the most promising approach to the creation of 1.3 μm -range VCSELs is the hybrid integration of the active region based on the InAlGaAsP-InP material system with semiconductor distributed



Bragg reflectors (DBR) GaAs/AlGaAs using the wafer fusion technology (WF-VCSEL) or with hybrid metal-dielectric mirrors based on high-contrast materials (HI-VCSEL) [2]. As the result of optimization of photon lifetime by variation of mirror losses and enhancement of differential gain by implementation of InAlGaAs quantum well active region the WF-VCSEL devices with the modulation bandwidth more than 12 GHz and error-free data transmission up to 10 km at 25 Gbps without any equalization technique were obtained [3]. As for the state-of-the-art HI-VCSEL, record modulation bandwidth more than 15 GHz [4] with the error-free data transmission at 30 Gbps over 10 km [5] and up to 50 Gbps [6] over 15 km without and with pre-equalization, respectively, were demonstrated for the devices with minimized mode volume (with shorter effective cavity length and smaller current aperture). Recently, we successfully tested the use of an InGaAs/InAlGaAs short-period superlattice (SL) as an active region of 1.3 μm -range WF-VCSELs [7,8].

In this paper, the results of studying the emission linewidth of 1.3 μm -range single-mode InGaAs SL-based WF-VCSEL are presented, and estimation of the α -factor is carried out.

Materials and Methods

WF-VCSEL designed in the geometry of a vertical microcavity with carrier injection through n -InP intracavity contacts and a composite tunnel junction (TJ) n^+ -InGaAs/ p^+ -InGaAs/ p^+ -InAlGaAs. For optical and current confinement, the concept of a buried tunnel junction (BTJ) was used, where mesas with 4 μm diameter were formed in the InGaAs layers of composite TJ. The active region was a short-period SL consisting of 24 pairs of $\text{In}_{0.57}\text{Ga}_{0.43}\text{As}/\text{In}_{0.53}\text{Ga}_{0.20}\text{Al}_{0.27}\text{As}$ layers with thicknesses of 0.8 and 2 nm accordingly [7]. A detailed description of the WF-VCSEL heterostructure and the fabrication of the WF-VCSEL chips are presented in [8]. After dicing into individual chips, the devices were mounted in TO-can package.

Results and Discussion

The investigation of WF-VCSELs demonstrated lasing with a threshold current of ~ 3 mA and a differential efficiency of ~ 0.68 W/A. Due to the laser self-heating effect, output optical power reached saturation at operating currents above 10 mA (Fig. 1,*a*). According to analysis of the emission spectra of the WF-VCSELs, those devices demonstrate lasing through the fundamental mode with a side-mode suppression ratio (SMSR) of more than 30 dB in the entire current range (Fig. 1,*b*). In addition, the polarization degeneracy of the fundamental mode was observed, which can be explained by the transverse asymmetry of BTJ mesa and/or the elasto-optical effect. Polarization-resolved study revealed the predominance of short wavelength mode with polarization along short axis of BTJ mesa with an orthogonal polarization suppression ratio (OPSR) of more than 20 dB in the entire operating range of currents and without the presence of polarization switching (Fig. 1,*a*).

To measure WF-VCSEL emission linewidth a SA30-144 scanning Fabry–Perot interferometer was used; a chemical current source was used to minimize noise, and an optical isolator was used to suppress optical feedback. According to the Schawlow-Townes-Henry theory, the emission linewidth of the semiconductor injection lasers could be described by the following equation, which considers the dependence of the refractive index on the carrier density [9]:

$$\Delta\nu = \frac{n_{sp}n_{SE}\bar{e}}{4\pi P_{out}n_j\tau_p^2}(1 + \alpha^2) + \Delta\nu_0, \quad (1)$$

where n_{sp} is the population inversion factor, n_{SE} is the slope efficiency, e is the elementary charge, P_{out} is the output optical power, n_j is the internal quantum efficiency, $\Delta\nu_0$ is the residual linewidth, τ_p is the photon lifetime.

According to Fig. 2, at first, the laser emission linewidth of the WF-VCSEL decreased inversely proportional with increase in the output optical power down to 40–45 MHz (at ~ 3.3 mW and operating current of ~ 8 mA). The linear approximation gives the value of the residual linewidth $\Delta\nu_0$ about 6.5 MHz, which can be associated with $1/f$ -noise (fluctuations of the charge carriers) and/or mode competition. However, with a further increase in the output optical power a broadening of the laser emission line could be observed, which, apparently, connected with the laser self-heating.

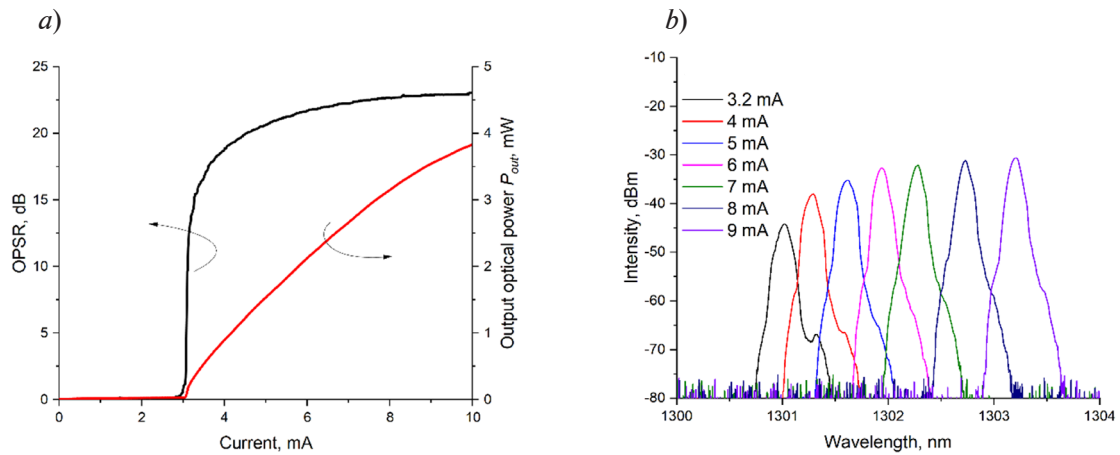


Fig. 1. Evolution of an output optical power with OPRS as functions of current (a) and optical spectra for different operating currents (b) measured at 20 °C

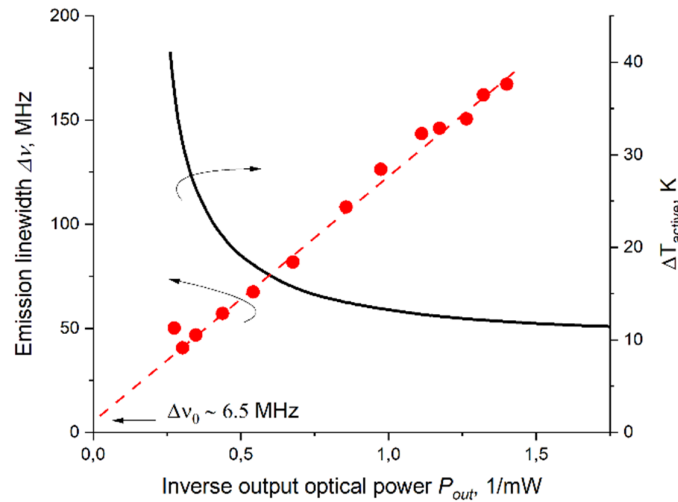


Fig. 2. Emission linewidth measured at 20 °C and the estimated internal laser temperature against inverse output optical power

With the intension to verify such assumption the study of the laser internal temperature was conducted. In accordance with [10], internal temperature rise of VCSELs could be evaluated as:

$$\Delta T_{int} = R_{th} (P_{diss} - P_{out}), \quad (2)$$

where R_{th} is the thermal resistance, P_{diss} is the dissipated electrical power.

Device R_{th} is defined by the resonance wavelength shifts with temperature $\Delta\lambda_0/\Delta T$ and with dissipated electrical power $\Delta\lambda_0/\Delta P_{diss}$. With the study of optical spectra for different operating current and different heat-sink temperatures the dissipated power shift $\Delta\lambda_0/\Delta P_{diss}$ at fixed heat-sink temperature T (Fig. 3,a) and the temperature shift $\Delta\lambda_0/\Delta T$ at fixed dissipated electrical power P_{diss} (Fig. 3,b) were evaluated as 0.22 nm/mW and 0.09 nm/°C accordingly. So, calculated thermal resistance value $R_{th} = (\Delta\lambda_0/\Delta P_{diss}) / (\Delta\lambda_0/\Delta T)$ was 2.46 °K/mW, which is significantly lower than thermal resistance of long-wavelength HI-VCSELs with the same BTJ mesa diameter [11]. It should be noted that such high calculated value of R_{th} compared with work [7] could be explained by higher P_{diss} value (lower slope efficiency) and peculiarities of chip packaging. As shown in Fig. 2, the sharp rise of laser internal temperature ΔT_{int} revealed for output optical power more than 2 mW (operating current over than 5.5 mA).

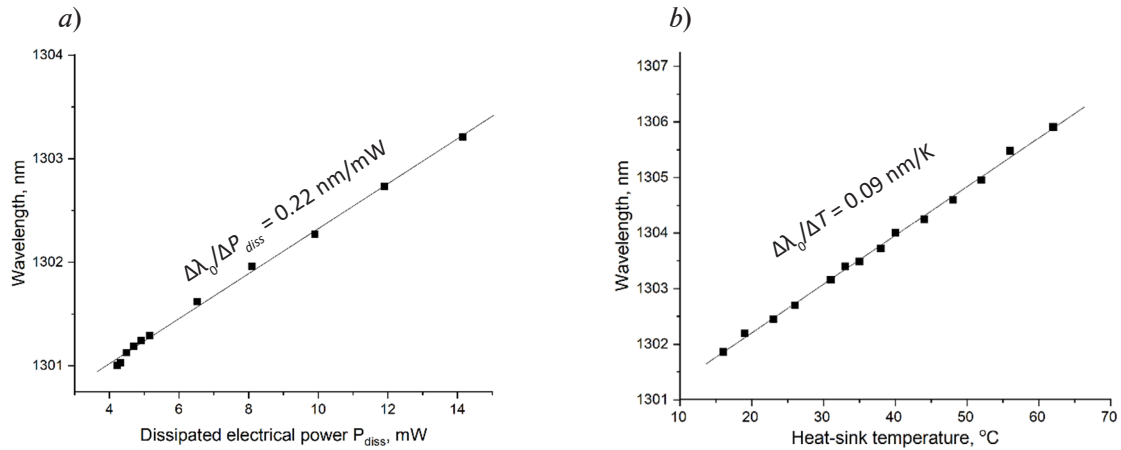


Fig. 3. Dependences of the wavelength shift on dissipated electrical power at fixed heat-sink temperature of 20 °C (a) and the wavelength shift on heat-sink temperature at fixed dissipated electrical power (b)

Dependence of photon lifetime in cavity on mirror losses T_m and internal optical losses A_{int} could be described as follows [9]:

$$\tau_p = 1 / \nu_g (T_m + A_{int}), \quad (3)$$

where ν_g is the group velocity ($\sim 10^{10}$ cm/s). Values of A_{int} and n_j were found from iterative varying of mirror losses by the deposition of the thin dielectric layer on the top DBR mirror as was conducted in [12]. According to Fig. 4., rise of heat-sink temperature leads to the increased internal optical losses of WF-VCSEL, which could be explained by stronger free-carrier absorption in the doped region and/or interband absorption in the InGaAs layers. As for the drop in the internal quantum efficiency, it may be due to the overflow of charge carriers as the threshold currents increase with temperature.

Note that the population inversion factor n_{sp} is difficult to determine separately from the α -factor. Using expressions (1) and (3) the value of the α -factor was estimated to be about 7.7–9 at 20 °C for n_{sp} in range 2–1.5, respectively.

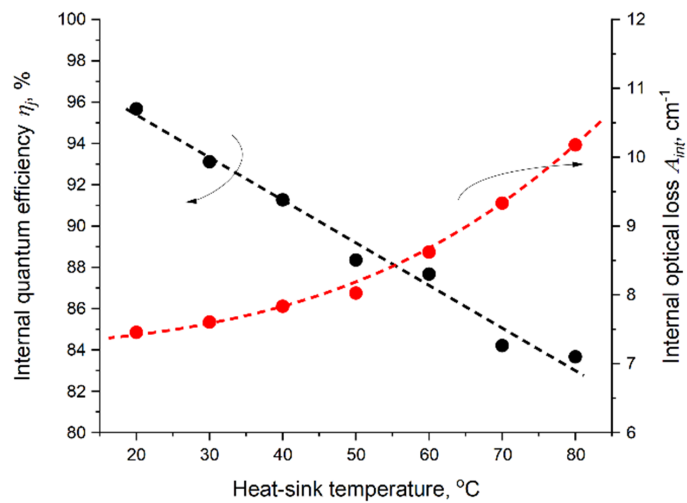


Fig. 4. Estimated internal quantum efficiency and internal optical losses as function of heat-sink temperature

Additionally, it can be observed that the gradual decrease in the internal quantum efficiency and the increase in the internal optical losses due to a rise in the laser internal temperature led to the decrease in the slope efficiency and the photon lifetime, which, according to expression (1), could potentially cause the laser emission linewidth broadening. However, it is more likely that the observed broadening is associated with the gain saturation at the higher operating currents and the decrease in the material gain at the higher laser internal temperature. Both effects led to the reduction of the differential gain at the higher carrier density and/or laser internal temperature [9], which finally resulted to the rise of the α -factor [13] despite the further increase in the output optical power [14].

Conclusion

In this work, we analyzed the emission linewidth of 1.3 μm -range InGaAs/InAlGaAs SL-based WF-VCSELs. For 20 °C, the linewidth drops to 45-40 MHz at 3.3 mW. The linewidth enhancement factor of 9–7.7 was estimated assuming population inversion factor of 2–1.5.

REFERENCES

1. **Padullaparthi B.D., Tatum J.A., Iga K.**, VCSEL industry: communication and sensing. Wiley-IEEE Press, 2021. 352 p.
2. **Babichev A., Blokhin S., Kolodeznyi E., Karachinsky L., Novikov I., Egorov A., Tian S.-C., Bimberg D.**, Long-Wavelength VCSELs: Status and Prospects // *Photonics*. 2023. Vol. 10, № 3. P. 268. 10.3390/photonics10030268.
3. **Caliman A., Sirbu A., Iakovlev V., Mereuta A., Wolf P., Bimberg D., Kapon E.**, 25 Gbps direct modulation and data transmission with 1310 nm waveband wafer fused VCSELs // *Optical Fiber Communication Conference*. Washington, D.C.: OSA, 2016. P. Tu3D.1. 10.1364/OFC.2016.Tu3D.1.
4. **Müller M., Grasse C., Saller K., Gründl T., Böhm G., Ortsiefer M., Amann M.C.**, 1.3 μm High-Power Short-Cavity VCSELs for High-Speed Applications // *Conference on Lasers and Electro-Optics 2012*. Washington, D.C.: OSA, 2012. P. CW3N.2. 10.1364/CLEO_SI.2012.CW3N.2.
5. **Spiga S., Müller M., Amann M.-C.**, Energy-efficient high-speed InP-based 1.3 μm short-cavity VCSELs // *2013 15th International Conference on Transparent Optical Networks (ICTON)*. IEEE, 2013. P. 1–4. 10.1109/ICTON.2013.6602683.
6. **Breyne L., Verplaetse M., Neumeys C., De Keulenaer T., Soenen W., Yin X., Ossieur P., Torfs G., Bauwelinck J.**, DSP-Free and Real-Time NRZ Transmission of 50 Gb/s Over 15-km SSMF and 64 Gb/s Back-to-Back With a 1.3- μm VCSEL // *J. Light. Technol.* 2019. Vol. 37, № 1. P. 170–177. 10.1109/JLT.2018.2885619.
7. **Blokhin S.A., Babichev A. V., Gladyshev A.G., Karachinsky L.Y., Novikov I.I., Blokhin A.A., Bobrov M.A., Maleev N.A., Andryushkin V. V., Denisov D. V., Voropaev K.O., Zhumaeva I.O., Ustinov V.M., Egorov A.Y., Ledentsov N.N.**, High Power Single Mode 1300-nm Superlattice Based VCSEL: Impact of the Buried Tunnel Junction Diameter on Performance // *IEEE J. Quantum Electron.* 2022. Vol. 58, № 2. P. 1–15. 10.1109/JQE.2022.3141418.
8. **Blokhin S., Babichev A., Gladyshev A., Karachinsky L., Novikov I., Blokhin A., Rochas S., Denisov D., Voropaev K., Ionov A., Ledentsov N., Egorov A.**, Wafer-fused 1300 nm VCSELs with an active region based on superlattice // *Electron. Lett.* 2021. Vol. 57, № 18. P. 697–698. 10.1049/ell2.12232.
9. **Coldren L.A., Corzine, S. W., Mashanovitch M.L.**, Diode lasers and photonic integrated circuits. John Wiley & Sons, 2012. 583 p.
10. **Michalzik R.**, VCSELs: Fundamentals, Technology and Applications of Vertical-Cavity Surface-Emitting Lasers // *Springer Series in Optical Sciences*. Springer Verlag, 2013. 10.1007/978-3-642-24986-0_2.
11. **Spiga S., Schoke D., Andrejew A., Boehm G., Amann M.-C.**, Effect of Cavity Length, Strain, and Mesa Capacitance on 1.5- μm VCSELs Performance // *J. Light. Technol.* 2017. Vol. 35, № 15. P. 3130–3141. 10.1109/JLT.2017.2660444.
12. **Blokhin S.A., Bobrov M. A., Blokhin A.A., Maleev N.A., Kuzmenkov A.G., Vasylyev A. P., Rochas S. S., Babichev A. V., Novikov I. I., Karachinsky L. Ya., Gladyshev A. G., Denisov D. V., Voropaev K. O., Egorov A. Yu., Ustinov V. M.**, Analysis of internal optical loss of 1.3 μm vertical-cavity surface-emitting laser based on n^{++} -InGaAs/ p^{++} -InGaAs/ p^{++} -InAlGaAs tunnel junction // *Tech. Phys. Lett.* 2022. Vol. 48, № 15. P. 3. 10.21883/TPL.2022.15.53808.18938.



13. Halbritter H., Riemenschneider F., Jacquet J., Provost J.-G., Symonds C., Sagnes I., Meissner P., Chirp and linewidth enhancement factor of tunable, optically-pumped long wavelength VCSEL // Electron. Lett. 2004. Vol. 40, № 4. P. 242. 10.1049/el:20040173.

14. Shau R., Halbritter H., Riemenschneider F., Ortsiefer M., Roskopf J., Buhm G., Maute M., Meissner P., Amann M.-C., Linewidth of InP-based 1.55 [micro sign]m VCSELs with buried tunnel junction // Electron. Lett. 2003. Vol. 39, № 24. P. 1728. 10.1049/el:20031143.

THE AUTHORS

KOVACH Yakov N.

j-n-kovach@itmo.ru

ORCID: 0000-0003-4858-4968

BLOKHIN Sergey A.

blokh@mail.ioffe.ru

ORCID: 0000-0002-5962-5529

BOBROV Mikhail A.

bobrov.mikh@gmail.com

ORCID: 0000-0001-7271-5644

BLOKHIN Alexey A.

bloalex91@yandex.ru

ORCID: 0000-0002-3449-8711

MALEEV Nikolai A.

Maleev@beam.ioffe.ru

ORCID: 0000-0003-2500-1715

KUZMENKOV Alexander G.

Kuzmenkov@mail.ioffe.ru

ORCID: 0000-0002-7221-0117

GLADYSHEV Andrey G.

andrey.gladyshev@connector-optics.com

ORCID: 0000-0002-9448-2471

NOVIKOV Innokenty I.

innokenty.novikov@itmo.ru

ORCID: 0000-0003-1983-0242

KARACHINSKY Leonid Ya.

leonid.karachinsky@connector-optics.com

ORCID: 0000-0002-5634-8183

VOROPAEV Kirill O.

kirill.voropaev@novsu.ru

ORCID: 0000-0002-6159-8902

EGOROV Anton Yu.

anton.egorov@connector-optics.com

ORCID: 0000-0002-0789-4241

USTINOV Victor M.

Vmust@beam.ioffe.ru

ORCID: 0000-0002-6401-5522

Received 30.06.2023. Approved after reviewing 31.07.2023. Accepted 01.08.2023.